Polyhedron 28 (2009) 1583–1593

Contents lists available at ScienceDirect

Polyhedron

journal homepage: www.elsevier.com/locate/poly

Coinage metal derivatives of salicylaldehyde thiosemicarbazones: Synthesis, structures, bond isomerism and H-bonded networks

Tarlok Singh Lobana [a,*], Sonia Khanna [a], Geeta Hundal [a], Pavneet Kaur [a], Bandana Thakur [a], Shaweta Attri [a], Ray Jay Butcher [b]

[a] Department of Chemistry, Guru Nanak Dev University, Amritsar 143005, India
[b] Department of Chemistry, Howard University, Washington, DC 20059, USA

ARTICLE INFO

Article history:
Received 3 February 2009
Accepted 19 March 2009
Available online 28 March 2009

Keywords:
Salicylaldehyde thiosemicarbazone
Bond isomerism
Halogen bridging
Sulfur bridging

ABSTRACT

Reactions of salicylaldehyde thiosemicarbazone {(2-HO–C_6H_4)(H)C^2=N^3–N^2H–C^1(=S)N^1H_2, H_2stsc} and salicylaldehyde N-methyl thiosemicarbazone {(2-HO–C_6H_4)(H)C^2=N^3–N^2H–C^1(=S)N^1HMe, H_2stscNMe} with copper(I)/silver(I) halides in presence of PPh_3 have yielded complexes of compositions, mononuclear [CuCl(η^1-S–Htsc)(PPh_3)$_2$] (Htsc = H_2stsc **3**; H_2stscNMe, **6**), [AgX(H_2stscNMe)(PPh_3)]$_2$ (Br **9**, Cl **10**), sulfur-bridged dimers, [Cu_2(μ-S–H_2stscNMe)$_2X_2$(PPh_3)$_2$] · 2CH_3CN (I **4**; Br **5**), [Ag_2Cl_2(μ-S–H_2stsc)$_2$(PPh_3)$_2$] **8** and bond isomers, [M_2X_2 (H_2stsc)$_2$(PPh_3)$_2$] (M: Cu I **1**, Br **2**; Ag **7**). Complexes **1**, **2** and **7** exist as halogen-bridged [M_2(μ-X)$_2$(η^1-S–H_2stsc)$_2$(PPh_3)$_2$] (M: Cu, **1a**, **2a**; Ag, **7a**), and sulfur bridged [M_2(μ-S–H_2stsc)$_2X_2$(PPh_3)$_2$] (M: Cu, **1b**, **2b**; Ag, **7b**) isomers in the same lattice. Among the bond isomers, the Cu···Cu contacts were found to be shorter in sulfur-bridged isomers (**1b**, 3.113; **2b**, 3.063 Å) vis-à-vis those in halogen bridged isomers (**1a**, 3.182; **2a**, 3.190 Å). The Ag···Ag contact in sulfur-bridged isomer **7b** (3.4223 Å) is longer than in bromo-bridged isomer **7a** (3.2021 Å). The complexes form 1D or 2D H-bonded networks, entrapping solvent molecules in some cases.

1. Introduction

An assembly of polymetallic systems can occur via coordinate bond formation (coordination polymers), and via hydrogen bonding or other weaker interactions (supramolecular 1D, 2D or 3D networks) [1,2]. The synthesis of coordination polymers has gained attention for the past several years, for their unique properties, and fascinating structures [1]. In recent years, several 1D, 2D or 3D polymers with conductivity and magnetic properties have been reported [3–6]. Supramolecular systems have shown interesting donor–acceptor interactions, leading to the design of new materials and new carriers for drug delivery resulting in great impact in the pharmaceutical sciences [7–10].

Thiosemicarbazones {$R^1R^2C^2$=N^3–N(H)–C^1(=S)N^1HR^3} possessing several donor atoms have shown propensity for the formation of mono-, di- and poly-nuclear complexes with transition metals [11–17]. These ligands have also displayed ion-sensing ability [18–21] metal extraction properties, [22,23] and pharmacological properties [24–28]. The presence of available hydrogen atoms in the thiosemicarbazones is important for the building of H-bonded networks [29,30]. Dinuclear copper metal complexes are very important due to their role in many copper proteins [31], electrolytic reduction of carbon dioxide [32], and other catalytic activities [33–35]. Further, the close M···M contacts in dimers are anticipated to promote photoluminiscent properties [36–38].

We have been interested in the importance of the substituents at C^2/N^1 atoms of thiosemicarbazones on the nature of bonding, nuclearity and H-bonded networks. In this paper, we report complexes of salicylaldehyde thiosemicarbazone (H_2stsc) and its N^1-methyl substituted ligand (H_2stscNMe) (Chart 1) which has generated 1D and 2D networks, several of which selectively entrap organic molecules in the voids between parallel chains.

2. Experimental

2.1. General material and techniques

Copper(I) halides were prepared by the reduction of $CuSO_4 \cdot 5H_2O$ using SO_2 in the presence of NaX (X = Cl, Br, I) in distilled water. Silver(I) halides were prepared by the reaction of silver(I) nitrate in methanol with NaX (X = Cl, Br) [39]. Thiosemicarbazide, N^1-methyl thiosemicarbazide, salicylaldehyde and Ph_3P were procured from Aldrich Sigma Ltd. Thiosemicarbazone ligands were prepared by condensation of aldehydes with respective thiosemicarbazides. Elemental analysis for C, H and N were carried out using a thermoelectron FLASHEA1112 analyser. The melting points were determined with a Gallenkamp electrically heated

* Corresponding author. Tel.: +91 183 22 57604; fax: +91 183 22 58820.
E-mail address: tarlokslobana@yahoo.co.in (T.S. Lobana).

0277-5387/$ - see front matter © 2009 Published by Elsevier Ltd.
doi:10.1016/j.poly.2009.03.019

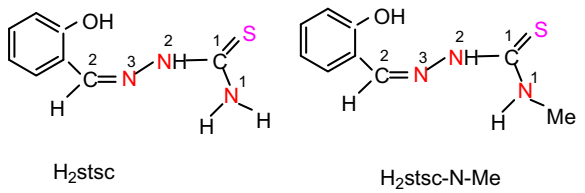

Chart 1.

apparatus. The I.R spectra of the ligands and the complexes were recorded in the range, 4000–200 cm^{-1} (using KBr pellets) on the FTIR-SHIMADZU 8400 Fourier Transform Spectrophotometer and on Pye-Unicam SP-3-300 spectrophotometer.

2.2. Synthesis of complexes

2.2.1. $[Cu_2I_2(H_2stsc)_2(PPh_3)_2] \cdot CHCl_3$ (**1**)

To copper(I) iodide (0.025 g, 0.131 mmol) in a mixture of acetonitrile (10 mL) and $CHCl_3$ (10 mL) was added H_2stsc ligand (0.025 g, 0.131 mmol), and the contents were stirred for 2 h, followed by the addition of PPh_3 (0.034 g, 0.131 mmol). The contents were stirred until a clear solution was obtained which was filtered, and kept for crystallization for 2–3 days, when yellow colored crystals were formed. Crystals were air sensitive and turned opaque when taken out of their mother liquor. Yield, 66%, 0.112 g, m.p. 200–202 °C. *Anal.* Calc. for $C_{52}H_{48}Br_2Cu_2N_6O_2P_2S_2 \cdot \frac{1}{2}CHCl_3$: C, 46.51; H, 3.58; N, 6.20. Found: C, 46.66; H, 3.43; N, 6.38%. IR data (KBr, cm^{-1}): (O–H) 3433(b); ν(N–H) 3306(m), 3277(s) (–NH_2–) 3163(m), 3124(m) (–NH–); ν(C–H) 3051(s); ν(C=N) + δNH_2 + ν(C=C) 1597(m), 1547(s), 1458(s); ν(C=S) 805(s), 845(s) (thioamide moiety); ν(C–N) 975(s), 1075(s) ν(P–C_{Ph}) 1095(s). ^{1}H NMR ($CDCl_3$, δ ppm): 6.80–7.45m (PPh_3 + N^1H_2 + Ph), 8.55s (–C^2H), 9.41s (OH). ^{31}P NMR ($CDCl_3$, δ ppm): 30.06 ppm, $\Delta\delta(\delta_{complex} - \delta_{ligand})$ = 34.78 ppm.

Complexes **2**–**6** were prepared similarly.

2.2.2. $[Cu_2Br_2(H_2stsc)_2(PPh_3)_2] \cdot CHCl_3$ (**2**)

Yield, 51%, 0.11 g, m.p. 210–212 °C. *Anal.* Calc. for $C_{52}H_{48}Br_2Cu_2N_6O_2P_2S_2 \cdot \frac{1}{2}CHCl_3$: C, 49.97; H, 3.84; N, 6.66. Found: C, 49.94; H, 4.10; N, 6.71%. IR data (KBr, cm^{-1}): ν(O–H) 3458(sb); ν(N–H) 3308(m), 3275(sh) (–NH_2–) 3159(s), 3130(m) (–NH–); ν(C–H) 3057(s), 2999(s); ν(C=N) + δNH_2 + ν(C=C) 1614(m), 1599(s), 1551(m); ν(C=S) 815(s) (thioamide moiety); ν(C–N) 1020(s), 970(s); ν(P–C_{Ph}) 1093(s). ^{1}H NMR ($CDCl_3$, δ ppm): 6.97–7.48m (Ph + PPh_3 + N^1H_2), 8.52s (–C^2H), 9.45s (OH). ^{31}P NMR ($CDCl_3$, δ ppm): −3.52 ppm, $\Delta\delta(\delta_{complex} - \delta_{ligand})$ = 1.19 ppm.

2.2.3. $[CuCl(\eta^1\text{-}S\text{–}H_2stsc)(PPh_3)_2] \cdot CH_3CN$ (**3**)

Yield, 52%, 0.110 g, m.p. 180–182 °C. *Anal.* Calc. for $C_{46}H_{42}ClCuN_4OP_2S$: C, 64.20; H, 4.88; N, 6.51. Found: C, 64.30; H, 4.69; N, 6.45%. IR data (KBr, cm^{-1}): ν(O–H) 3470(s); ν(N–H) 3350(m) (–NH_2–) 3197(s), 3150(s) (–NH–); ν(C–H) 3055(s), 2980(s); ν(C=N) + δNH_2 + ν(C=C) 1595(m), 1543(s); ν(C=S) 835(s) (thioamide moiety); ν(C–N) 1020(s); ν(P–C_{Ph}) 1095(s). ^{1}H NMR ($CDCl_3$, δ ppm): 6.07b (–N^1H_2), 6.91–7.46m (PPh_3 + N^1H_2), 8.28s (–C^2H), 9.56s (OH), 12.90s (–N^2H). ^{31}P NMR ($CDCl_3$, δ ppm): −2.97 ppm, $\Delta\delta(\delta_{complex} - \delta_{ligand})$ = 1.74 ppm.

2.2.4. $[Cu_2I_2(\mu\text{-}S\text{–}H_2stscNMe)_2(PPh_3)_2] \cdot CH_3CN$ (**4**)

Yield, 73%, 0.06 g, m.p. 150–152 °C. *Anal.* Calc. for $C_{54}H_{52}I_2Cu_2N_6P_2S_2$: C, 53.4; H, 4.9; N, 8.7. Found: C, 53.2; H, 4.8; N, 8.3%. Main IR peaks (KBr, cm^{-1}): ν(N^1–H) 3367m, 3242sh (–N^1H–), 3106b, 3093b (–N^2H–); 2958sh ν(C–H); 2806s, 2780s ν(N^1–CH_3); 1662s, 1618s, 1560m ν(C=N) + ν(C=C); 952s, 813s (thioamide moiety); 1093s ν(P–C_{Ph}). ^{1}H NMR ($CDCl_3$, δ ppm) 9.40b(–OH), 8.61s (–C^2H), 7.25–7.54m (Ph + PPh_3), 6.96q (–N^1H), 3.19s, 3.20s (–N^1–CH_3). ^{31}P NMR ($CDCl_3$, δ ppm): −143.0, $\Delta\delta(\delta_{complex} - \delta_{ligand})$ = 2.54 ppm.

2.2.5. $[Cu_2Br_2(\mu\text{-}S\text{–}H_2stscNMe)_2(PPh_3)_2] \cdot CH_3CN$ (**5**)

Yield, 60%, 0.064 g, m.p. 164–166 °C. *Anal.* Calc. for $C_{54}H_{52}Br_2Cu_2N_6P_2S_2)_2$: C, 36.6; H, 3.8; N, 11.2. Found: C, 36.2; H, 3.4; N, 11.4%. Main IR peaks (KBr, cm^{-1}): ν(N^1–H) 3396m, 3357m (–N^1H–), 3159s (–N^2H–); 3002s ν(C–H); 2788s ν(N^1–CH_3); 1618s, 1571s, 1521s ν(C=N) + ν(C=C); 1028s, 813s (thioamide moiety); 1093s ν(P–C_{Ph}). ^{1}H NMR ($CDCl_3$, δ ppm) 9.46b (–OH), 8.61s (–C^2H), 7.25–7.50m (Ph + PPh_3), 6.94q (–N^1H), 2.02d (–N^1–CH_3). ^{31}P NMR ($CDCl_3$, δ ppm): −143.04, $\Delta\delta(\delta_{complex} - \delta_{ligand})$ = 2.54 ppm.

2.2.6. $[CuCl(\eta^1\text{-}S\text{–}H_2stscNMe)(PPh_3)_2] \cdot CH_3CN$ (**6**)

Yield, 68%, 0.14 g, m.p. 182–184 °C. *Anal.* Calc. for $C_{47}H_{44}ClCuN_4SOP_2$: C, 64.60; H, 5.04; N, 6.41. Found: C, 65.1; H, 5.35; N, 6.65%. Main IR peaks (KBr, cm^{-1}): ν(N^1–H) 3392m, 3345m (–N^1H–), 3165s (–N^2H–); 2988s ν(C–H); 2780s ν(N^1–CH_3); 1628s, 1575s ν(C=N) + ν(C=C); 1025s, 820s (thioamide moiety); 1095s ν(P–C_{Ph}). ^{1}H NMR ($CDCl_3$, δ ppm) 9.47b (–OH), 8.65s (–C^2H), 7.28–7.47m (Ph + PPh_3), 6.98q (–N^1H), 2.03d (–N^1–CH_3). ^{31}P NMR ($CDCl_3$, δ ppm): −3.87 ppm, $\Delta\delta(\delta_{complex} - \delta_{ligand})$ = 0.84 ppm.

2.2.7. $[Ag_2Br_2(H_2stsc)_2(PPh_3)_2] \cdot 2CH_3CN$ (**7**)

To silver(I) bromide (0.025 g, 0.133 mmol) suspended in acetonitrile (15 mL) was added ligand H_2stsc (0.026 g, 0.133 mmol), and stirring was continued for 24 h. To the white solid formed, was added solid PPh_3 (0.035 g, 0.133 mmol), resulting in turbid solution. Addition of another mole of PPh_3 (0.035 g, 0.133 mmol) resulted in the formation of a clear solution, which was kept for crystallization. Slow evaporation of the solution resulted in two products, $[Ag_4Br_4(PPh_3)_4]$ and $[AgBr(H_2stsc)(PPh_3)]_2$ (**5**). The data for **5** is given. Yield, 0.04 g, 48%, m.p. 200–202 °C. *Anal.* Calc. for $C_{52}H_{48}Ag_2Br_2N_6O_2P_2S_2$: C, 48.39; H, 3.72; N, 6.51. Found: C, 48.14; H, 3.77; N, 6.53%. IR data (KBr, cm^{-1}): ν(O–H) 3450(b), ν(N–H) 3300(sh), 3298(b) (–NH_2–), 3153(m) (–NH–); ν(C–H) 3050(m), 3000(w); ν(C=N) + δNH_2 + ν(C=C) 1597(m), 1533(s), 1477(s); ν(C=S) 820(s) (thioamide moiety); ν(C–N) 960(s); ν(P–C_{Ph}) 1095(s). ^{1}H NMR ($CDCl_3$, δ ppm): 12.44sb (–N^2H), 11.66s (OH), 8.51s (–C^2H), 8.21sb, 7.85sb (–N^1H_2), 6.79–7.49m (Ph + PPh_3). ^{31}P NMR ($CDCl_3$, δ ppm): 29.8, −9.1 ppm, $\Delta\delta(\delta_{complex} - \delta_{ligand})$ = 34.4, 13.5 ppm.

2.2.8. $[Ag_2Cl_2(\mu\text{-}S\text{–}H_2stsc)_2(PPh_3)_2]$ (**8**)

To silver(I) chloride (0.025 g, 0.174 mmol) suspended in acetonitrile (15 mL) was added solid PPh_3 (0.045 g, 0.174 mmol), and the contents were stirred for 24 h. The white solid formed was filtered and dried in vacuo. To this solid (0.050 g, 0.123 mmol), suspended in methanol, was added H_2stsc ligand (0.024 g, 0.123 mmol) and the contents were stirred until a clear solution was obtained which was filtered, and kept for crystallization for 2–3 days, when pale yellow crystals were formed. Yield, 64%, 0.134 g, m.p. 216–218 °C. *Anal.* Calc. for $C_{54}H_{52}Ag_2Cl_2N_6P_2S_2O_2$: C, 54.15; H, 4.34; N, 7.02. Found: C, 53.89; H, 4.83; N, 7.28%. IR data (KBr, cm^{-1}): ν(O–H) 3433(sb); ν(N–H) 3306(sh), 3277(b) (–NH_2–) 3163(m), 3125(b) (–NH–); ν(C–H) 3051(s); ν(C=N) + δNH_2 + ν(C=C) 1596(s), 1547(s), 1458(s); ν(C=S) 830(s), 815(s); ν(C–N) 1050(sb), 955(s); ν(P–C_{Ph}) 1095(s). ^{1}H NMR ($CDCl_3$, dmso–d_6, δ ppm): 7.24–7.57m (N^1H_2 + Ph + PPh_3), 7.87sb (–N^1H_2), 8.57s (–C^2H), 9.50s (OH), 12.03s (–N^2H). ^{31}P NMR ($CDCl_3$, dmso–d_6, δ ppm): −8.72 ppm, $\Delta\delta(\delta_{complex} - \delta_{ligand})$ = 13.37 ppm.

2.2.9. $[AgBr(\eta^1\text{-}S\text{–}H_2stsc\text{–}N\text{–}Me)(PPh_3)_2] \cdot 3CH_3CN$ (**9**)

To silver(I) bromide (0.025 g, 0.13 mmol) suspended in acetonitrile (15 mL) was added ligand H_2stscNMe (0.027 g, 0.13 mmol),

and stirring was continued for 24 h. To the white solid formed, was added solid PPh_3 (0.034 g, 0.13 mmol), resulting in turbid solution. Addition of another mole of PPh_3 (0.034 g, 0.13 mmol) resulted in the formation of a clear solution, which was kept for crystallization. Slow evaporation of the solution resulted in formation of white transparent crystals. Crystals were stored in mother liquor. Yield, 71%, 0.087 g, m.p. 165–167 °C. *Anal.* Calc. for $C_{43}H_{41}AgBrN_3OP_2S$: C, 58.6; H, 4.5; N, 4.4. Found: C, 58.8; H, 5.5; N, 4.5%. IR data (KBr, cm^{-1}): ν(NH) 3307(s), 3216(s); (–N^1H–) 3142(s), (–N^1–CH_3) 2775(b); ν(C–H) 3049(s); ν(C=N) + ν(C=C) 1603(s), 1558(s), 1510(s), ν(C=S) 822(s); ν(C–N) 1078(s), 951(m); ν(P–C_{Ph}) 1094(s). ^{1}H NMR ($CDCl_3$, δ ppm): 11.74s (–N^2H); 8.60s (–C^2H); 7.26–7.49m (PPh_3), 6.974–6.90m (–$C^{6,7,8}$H); 3.16s, 3.15s (–N^1–CH_3). ^{31}P NMR ($CDCl_3$, δ ppm): −5.4 ppm, $\Delta\delta(\delta_{complex} - \delta_{ligand})$ = 10.05 ppm.

Complex **10** was prepared similarly.

*2.2.10. [AgCl(η^1-S–H_2stscNMe)(PPh_3)$_2$] · 3CH_3CN (**10**)*

Yield, 68%, 0.113 g, m.p. 172–174 °C. *Anal.* Calc. for $C49H_{47}AgClN5OP_2S$: C, 61.34; H, 4.9; N, 7.3. Found: C, 61.51; H, 4.7; N, 7.1%. IR data (KBr, cm^{-1}): ν(O–H) 3647(s); ν(NH) 3308(s), 3288(s); (–N^1H–) 3138(s), 3113(s) (–N–H); ν(C–H) 3070(s), 3051(s); (–N^1–CH_3) 2986(m), 2949(m); ν(C=N) + ν(C=C) 1558(s), 1526(s), 1481(s); ν(P–C_{Ph}) 1093(s); ν(C–N) 1078(s), 1028(m); ν(C=S) 854(s), 823(s). ^{1}H NMR ($CDCl_3$, δ ppm): 12.10s (–N^2H); 9.57s (–C^2H); 8.55s (OH); 7.28–7.40m (Ph + PPh_3), 6.92q (–N^1H); 3.18d (–N^1–CH_3). ^{31}P NMR ($CDCl_3$, δ ppm): −5.1 ppm, $\Delta\delta(\delta_{complex} - \delta_{ligand})$ = 9.8 ppm.

3. Crystal structure determination

The data for **1**–**6** were collected on a Siemens P4 diffractometer using XSCANS [40]. The θ–2θ technique was used to measure the intensities, up to a maximum of 2θ = 50°, with graphite monochromatised Mo Kα radiator (λ = 0.71073 Å). The data were corrected for Lorentz and polarization factors. An empirical psi absorption correction was applied. The structures were solved by direct methods and refined by full matrix least squares methods based on F^2. Hydrogen atoms were fixed geometrically and were not refined. Scattering factors from the International Tables for X-ray crystallography were used [41]. Data reduction, structure solution, refinement and molecular graphics were performed using SHELXTL-PC [42] and WINGX [43]. As the chloroform molecule in compound **2** is a disordered molecule, it shows a short distance between C5···Cl3, 2.48 Å.

The data for **10** was measured on Bruker AXS SMART APEX CCD diffractometer. Data were reduced and corrected for absorption using SMART and SAINT [44]. The structures were solved by direct methods and refined by full matrix least squares based on F^2 with anisotropic thermal parameters for non-hydrogen atoms using SHELXTL (structure solution, refinement and some molecular graphics). All non-hydrogen atoms were refined anisotropically. All hydrogen atoms were placed in calculated positions and were refined with an isotropic displacement parameter 1.5 (methyl) or 1.2 times (all others) that of the adjacent carbon or oxygen atom.

A prismatic crystal of complex (**7**–**9**) were mounted on an Bruker Apex 2 CCD area detector (**7**) or Oxford Diffraction Gemini-R (**8**, **9**) diffractometer equipped with a graphite monochromator, and Mo Kα radiation (λ = 0.71073 Å). The structures were solved by the direct methods and refined by full matrix least square based on F^2 with anisotropic thermal parameters for non-hydrogen atoms using XCAD-49 (data reduction), and SHELXL (absorption correction, structure solution refinement and molecular graphics) [45].The structure solutions for **7** showed disorder in the hydroxyl groups of the salicylaldehyde units, being spread at two ortho positions with respect to the pivot C bearing the imine group. This disorder was resolved by splitting the respective oxygen atoms at two ortho positions with total site occupancy of one. The H atoms were calculated in structure factor calculations in their idealized positions.

4. Results and discussion

4.1. General comments

Salicylaldehyde thiosemicarbazone and its N^1-methyl substituted ligands were reacted with copper(I) halides and silver(I) ha-

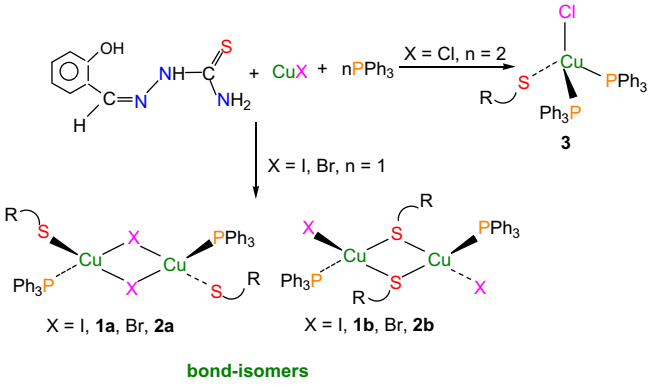

Scheme 1.

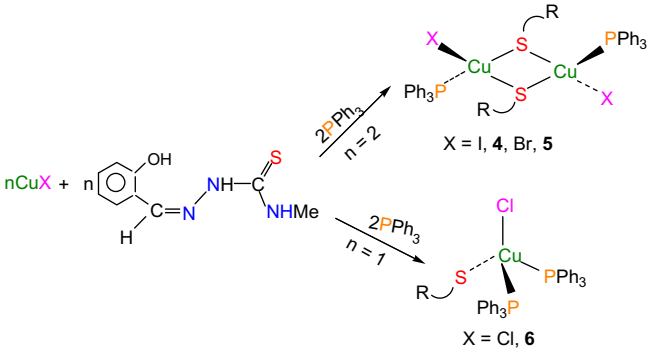

Scheme 2.

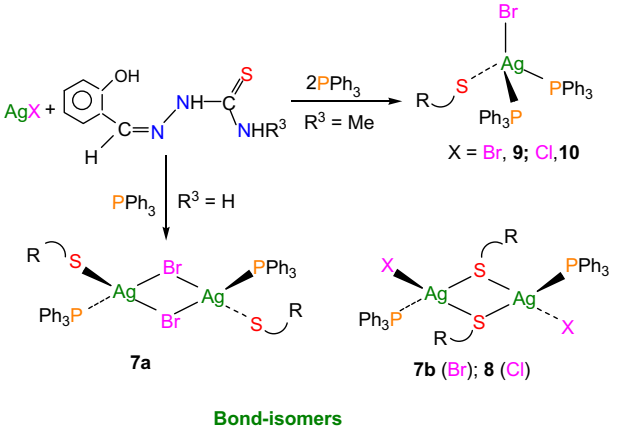

Scheme 3.

Table 1
Crystallographic data of complexes **1**–**10**.

Compound	**1**	**2**	**3**	**4**	**5**	**6**	**7**	**8**	**9**	**10**
Empirical formula	$C_{53}H_{49}Cl_3CuI_2N_6O_2P_2S_2$	$C_{53}H_{49}Br_2Cl_3Cu$-$N_6O_2P_2S_2$	$C_{46}H_{42}ClCuN_4OP_2S$	$C_{56}H_{56}Cu_2I_2N_8O_2P_2S_2$	$C_{58}H_{58}Cu_2Br_2N_8O_2P_2S_2$	$C_{47}H_{44}ClCuN_4OP_2S$	$C_{56}H_{54}Ag_2Br_2N_8O_2P_2S_2$	$C_{52}H_{48}Ag_2Cl_2N_6O_2P_2S_2$	$C_{51}H_{50}AgBrN_6OP_2S$	$C_{51}H_{50}AgClN_6OP_2S$
Molecular weight	1415.27	1321.9	859.83	1406.06	1312.10	873.85	1372.68	1201.66	1044.75	1000.29
Crystal system	triclinic	triclinic	triclinic	triclinic	triclinic	triclinic	triclinic	triclinic	triclinic	triclinic
T (K)	296(2)	296(2)	296(2)	293(2)	295(2)	295(2)	103(2)	293(2)	200(2)	100(2)
Space group	$P\bar{1}$	$P\bar{1}$	$P\bar{1}$	$P\bar{1}$	$P\bar{1}$	$P\bar{1}$	$P\bar{1}$	$P\bar{1}$	$P\bar{1}$	$P\bar{1}$
a (Å)	13.335(5)	13.367(2)	11.478(5)	10.907(5)	11.023(5)	11.132(1)	13.2196(7)	13.1828(8)	12.6245(7)	12.5853(13)
b (Å)	13.706(5)	13.630(2)	13.311(5)	11.792(5)	11.691(5)	13.620(1)	13.9888(7)	13.6503(15)	13.1974(6)	13.0318(13)
c (Å)	17.858(5)	17.613(2)	16.482(5)	13.601(5)	13.484(5)	17.191(1)	17.2767(9)	16.5090(19)	17.1534(7)	16.9636(17)
α (°)	77.650(5)	78.47(1)	76.550(5)	71.131(5)	100.276(5)	69.37(1)	82.150(1)	82.967(9)	80.698(4)	80.7420(10)
β (°)	72.350(5)	72.32(1)	78.910(5)	81.855(5)	98.682(5)	77.62(1)	73.230(1)	78.191(8)	81.042(4)	80.6590(10)
γ (°)	68.710(5)	69.43(1)	65.170(5)	63.969(5)	117.343(5)	66.67(1)	69.416(1)	63.116(10)	62.281(5)	62.2520(10)
V (Å^3)	2878.1(17)	2846.8(7)	2209.9(14)	1487.4(11)	1463.9(11)	2231.4(3)	2861.5(3)	2592.1(4)	2486.1(2)	2418.0(4)
Z	2	2	2	2	1	2	4	2	2	2
D_{calc} (Mg mm^{-1})	1.633	1.541	1.292	1.570	1.488	1.301	1.591	1.540	1.396	1.374
μ (mm^{-1})	2.124	2.466	0.713	1.925	2.266	0.707	2.258	1.047	1.358	0.625
Goodness of fit (GOF) on F^2	1.066	0.810	1.009	1.159	0.936	1.469	1.035	0.982	1.052	1.069
Largest difference in peak and hole (e Å^{-3})	0.711 and −0.979	0.623 and −0.798	0.768 and −0.463	0.629 and −0.547	0.679 and −0.961	1.857 and −3.354	0.643 and −1.022	1.049 and −0.597	1.835 and −0.872	0.724 and −0.520
R_1, wR_2 [$I > 2\sigma(I)$]	0.0666, 0.1514	0.0640, 0.1548	0.0811, 0.1689	0.0364, 0.0977	0.0443, 0.1107	0.0879, 0.2501	0.02228, 0.0561	0.0261, 0.0599	0.0778, 0.1677	0.0257, 0.0683
R_1, wR_2 (all data)	0.1235, 0.1847	0.1875, 0.2058	0.2063, 0.2372	0.0557, 0.1202	0.0822, 0.1416	0.1432, 0.3585	0.0278, 0.0585	0.0434, 0.0636	0.1621, 0.2239	0.0290, 0.0743

lides in the presence of triphenylphosphine, yielding a number of compounds (**1**–**10**) with variable nuclearities and bridging patterns Direct reactions of copper(I) halides with thiosemicarbazones generally yielded insoluble products, which could not be crystallized and triphenylphosphine was necessary for obtaining crystalline products. Two procedures were adopted for the preparation of complexes. One procedure involves reaction of a metal halide with a thiosemicarbazone followed by the addition of PPh_3, and second procedure involves first reaction of a metal halide with PPh_3, and then with a thiosemicarbazone. IR spectroscopy of all the complexes confirmed the presence of the individual ligands via their ν(N–H), ν(C–H)$_{Me}$, ν(C–N), ν(C=C), ν(C=N), ν(O–H) and ν(P–C) vibrational modes. The ν(C=S) thioamide bands are located at 805–854 cm^{-1}, which suggests (in agreement with the X-ray data) that a significant weakening of the C=S double bond occurs in all complexes.

Reactions of copper(I) halides with benzaldehyde thiosemicarbazone (R^1 = Ph, R^2 = R^3 = H; Hbtsc) in the presence of triphenylphosphine yield tetra-coordinated mononuclear [CuX(η^1-S–Hbtsc)$(Ph_3P)_2$] (X = I, Br), and dinuclear bromo-bridged [$Cu_2(\mu$-$Br)_2(\eta^1$-S–Hbtsc$)_2(Ph_3P)_2$], and sulfur-bridged [$Cu_2(\eta^1$-$Cl)_2(\mu$-S–Hbtsc$)_2$ $(Ph_3P)_2] \cdot 2CH_3CN$ complexes in acetonitrile [29,30]. Introduction of 2-hydroxyl phenyl group (R^1) at C^2 carbon (R^1 = 2-HO–C_6H_4, R^2, R^3 = H, H_2stsc) has completely changed the bonding and nuclearity pattern of the resulting complexes. For X = Cl, a tetra-coordinated mononuclear complex, [CuCl(η^1-S–H_2stsc$)(Ph_3P)_2] \cdot CH_3CN$ **3**, and for X = Br, I, dinuclear complexes, $[Cu_2X_2(H_2stsc)_2$- $(Ph_3P)_2] \cdot CHCl_3$ (X = I, **1**; Br, **2**) have been ob-

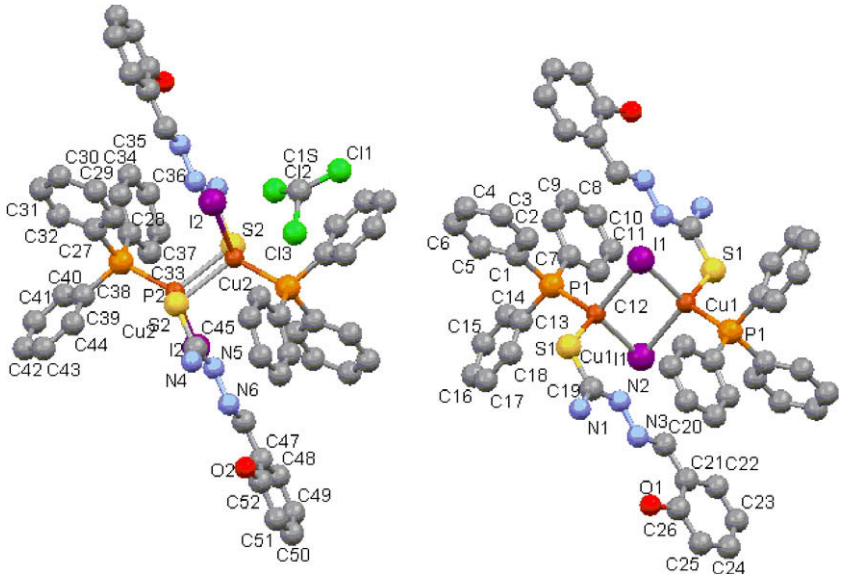

Fig. 1. Molecular structures of two crystallographically independent molecules of $[Cu_2I_2(H_2stsc)_2(PPh_3)_2] \cdot CHCl_3$ **1** in the unit cell (hydrogen atoms are removed for clarity; complex **2** has a similar structure).

Table 2
Important bond distances (Å) and bond angles (°) for complexes **1–6** with other related compounds.

Complex no.	Cu–S	Cu–X	Cu–P	Cu–X–Cu	X–Cu–X	Cu···Cu
Halogen-bridged dimers						
1a[a]	2.334(2)	2.6655(14) 2.7448(15) (I)	2.268(2)	72.02(4)	107.98(4)	3.182
2a[a]	2.303(2)	2.4932(16) 2.6328(18) (Br)	2.240(3)	76.91(5)	103.09(5)	3.190
				Cu–S–Cu	S–Cu–S	
Sulfur-bridged dimers						
1b[a]	2.328(2) 2.585(3)	2.6144(14) (I)	2.255(2)	78.46(8)	101.54(8)	3.113
2b[a] (Br)	2.316(3) 2.606(3)	2.4387(19) (Br)	2.244(3)	76.73(9)	103.27(9)	3.063
4[b]	2.3718(17) 2.4745(16)	2.6171(10) (I)	2.2650(14)	77.09(4)	102.91(4)	3.0211(15)
5[b]	2.3707(17) 2.4945(16)	2.3707(17) (Br)	2.2511(15)	75.49(6)	104.51(6)	2.9798(19)
Mononuclear complexes						
	Cu–P	Cu–Cl	Cu–S	P–Cu–P	P–Cu–S	P–Cu–Cl
3[a]	2.281(2) 2.294(2)	2.433(3)	2.387(3)	126.43(9)	103.59(9) 107.56(10)	100.46(9) 106.99(9)
6[b]	2.2780(18) 2.288(2)	2.453(2)	2.367(2)	123.68(7)	108.22(7) 112.12(8)	102.01(7) 102.02(7)

[a] H_2stsc.
[b] H_2stscNMe.

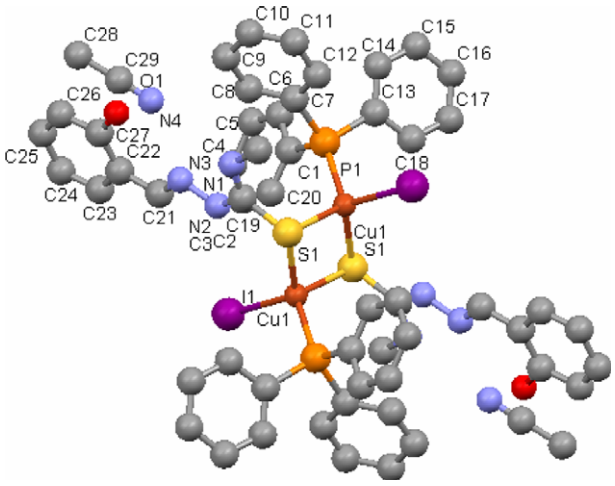

Fig. 2. Molecular structure of $[Cu_2I_2(\mu\text{-}S\text{–}H_2stscNMe)_2(PPh_3)_2] \cdot 2CH_3CN$ **4** (complex **5** has a similar structure).

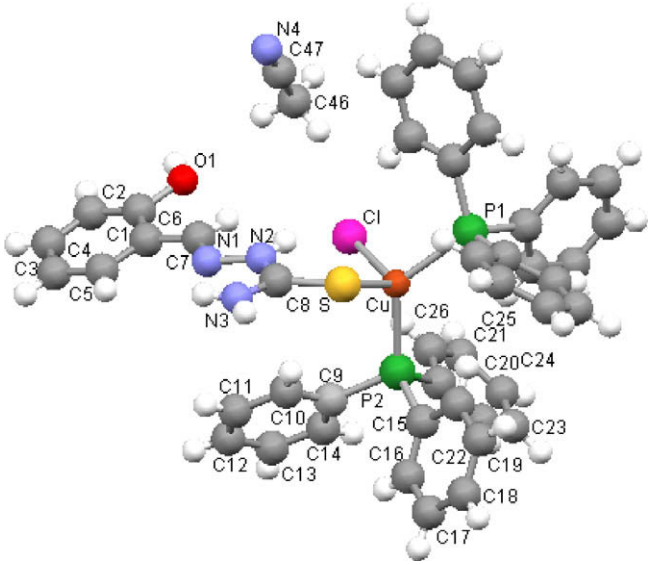

Fig. 3. Molecular structure of $[CuCl(\eta^1\text{-}S\text{–}H_2stsc)(PPh_3)_2] \cdot CH_3CN$ **3** with atomic numbering scheme (compound **6** has a similar structure).

tained (Scheme 3). Interestingly, **1** and **2** have both halogen-bridged (**1a**, **2a**), and sulfur-bridged (**1b**, **2b**) dinuclear species in their respective unit cells (Scheme 1). This phenomenon of bond isomerism is unprecedented in metal–thiosemicarbazone chemistry. In the preparation of **1**–**3** complexes, the addition of chloroform facilitated completion of reaction, which was partial in acetonitrile.

The introduction of methyl substituent (R^3) at N^1 (R^1 = 2-HO–C_6H_4, R^2 = H, R^3 = Me, H_2stscNMe) has yielded only sulfur-bridged dinuclear complexes, $[Cu_2(\eta^1\text{-}X)_2(\mu\text{-}S\text{–}H_2stscNMe)_2(Ph_3P)_2] \cdot CH_3CN$ (X = I, **4**; Br, **5**), unlike bond isomers observed in **1** or **2**. Copper(I) chloride has formed a mononuclear complex, $[CuCl(\eta^1\text{-}S\text{–}H_2stscNMe)(Ph_3P)_2] \cdot CH_3CN$ **6** similar to **3** (Scheme 2). Thus the behavior of H_2stsc and H_2stscNMe towards copper(I) chloride is similar but different for copper(I) bromide/iodide.

In order to check the generality of bond isomerism in coinage metals exhibited by H_2stsc, reactions were extended to silver(I) halides (X = Br, Cl). Silver(I) bromide with H_2stsc has formed a dinuclear complex, $[Ag_2Br_2(H_2stsc)_2(Ph_3P)_2] \cdot 2CH_3CN$ **7**, whose crystal structure revealed that it has bromo-bridged $[Ag_2(\mu\text{-}Br)_2(\eta^1\text{-}S\text{–}H_2stsc)_2(Ph_3P)_2]$ **7a** and sulfur-bridged, $[Ag_2(\eta^1\text{-}Br)_2(\mu\text{-}S\text{–}H_2stsc)_2(Ph_3P)_2]$ **7b** moieties in same unit cell, thus exhibiting bond isomerism similar to **1** or **2** (Scheme 3). Silver(I) chloride with H_2stsc did not react in CH_3CN (or CH_3CN/CH_3OH), and thus first silver(I) chloride was reacted with PPh_3 followed by the reaction with H_2stsc which yielded a sulfur-bridged dimer, $[Ag_2(\eta^1\text{-}Cl)_2(\mu\text{-}S\text{–}H_2stsc)_2(Ph_3P)_2]$ **8**, with no bond isomerism unlike that in **7**. It is pointed out here that Hbtsc with silver(I) bromide did not exhibit bond isomerism [17]. Further, introduction of a methyl group at N^1 (R^3) atom did not exhibit bond isomerism similar to **7**, rather mononuclear complexes, $[AgBr(\eta^1\text{-}S\text{–}H_2stscNMe)(Ph_3P)_2] \cdot 3CH_3CN$ **9** and $[AgCl(\eta^1\text{-}S\text{–}H_2stscNMe)(Ph_3P)_2] \cdot 3CH_3CN$ **10**, were obtained.

Bond isomerism in Cu/Ag complexes occurred only for R^1 = 2-OH–C_6H_4 with $R^2 = R^3$ = H only (**1**, **2**, **7**) and introduction of substituents at N^1 either prevented this isomerism or changed the nuclearity.

4.2. Crystal structures of complexes (*1*–*10*)

The crystal structures of all the complexes (**1**–**10**) have been obtained and crystal data are given in Table 1. All the complexes crystallized in triclinic system with $P\bar{1}$ space group.

The X-ray crystal structures of complexes of salicylaldehyde thiosemicarbazone (H_2stsc, R^1 = 2-HO–C_6H_4, $R^2 = R^3$ = H) with copper(I) halides have shown that each of dinuclear complexes,

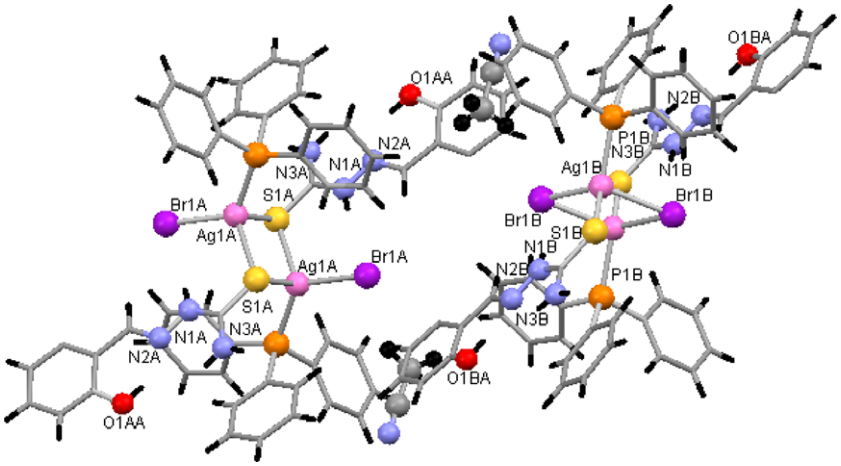

Fig. 4. Molecular structure of $[Ag_2Br_2(H_2stsc)_2(PPh_3)_2] \cdot 2CH_3CN$ (**7**) depicting bond isomers (**7a** and **7b**).

$[Cu_2X_2(H_2stsc)_2(PPh_3)_2]$. $CHCl_3$ (X = I **1**, Br **2**), co-exist as halogen bridged $[Cu_2(\mu\text{-}X)_2(\eta^1\text{-}S\text{–}H_2stsc)_2(PPh_3)_2]$ (I **1a**, Br **2a**) and sulfur bridged $[Cu_2X_2(\mu\text{-}S\text{–}H_2stsc)_2(PPh_3)_2]$ (I **1b**, Br **2b**) dimeric moieties in the same unit cell (bond isomers, Fig. 1). The central cores, $Cu(\mu\text{-}X)_2Cu$, of **1a** and **2a**, and $Cu(\mu\text{-}S)_2Cu$, of **1b** and **2b**, have unequal Cu–X or Cu–S distances and form parallelograms (Table 2). The Cu···Cu distances in halogen bridged dimers **1a**/**2a** are somewhat longer than those in the iodo-bridged dimers in literature. Likewise, the Cu···Cu separation in the sulfur bridged moieties **1b**/**2b** is marginally shorter than in halogen bridged moieties (**1a**, **2a**). When methyl group was attached at N^1 atom, there was no bond isomerism, and the Cu···Cu contacts decrease in the sulfur-bridged dimers, $[Cu_2X_2(\mu\text{-}S\text{–}H_2stscNMe)_2(PPh_3)_2]\cdot 2CH_3CN$ (X: I, **4** (Fig. 2), Br, **5**) versus those in similar dimeric units **1b** and **2b**. There is a marginal effect on Cu–P distances as well as on Cu–S–Cu and S–Cu–S angles with methyl substitution at N^1 atom. The angles at copper or halogen/ sulfur atoms of the central $Cu(\mu\text{-}X)_2Cu$ and $Cu(\mu\text{-}S)_2Cu$ cores vary in the complementary fashion (Table 2).

Both copper(I) chloride complexes with the ligands H_2stsc and $H_2stscNMe$, namely, $[CuCl(\eta^1\text{-}S\text{–}Htsc)(PPh_3)_2]$ {**3** (Fig. 3), **6**} have distorted tetrahedral structures. The substitution of methyl group at N^1 results in the marginal changes in Cu–Cl, Cu–S bond distances and P–Cu–P, P–Cu–S bond angles (Table 2).

As regards silver(I), salicylaldehyde thiosemicarbazone (H_2stsc) with silver(I) bromide has formed a dinuclear complex, $[Ag_2Br_2(H_2stsc)_2(PPh_3)_2]\cdot 2CH_3CN$ (**7**), co-existing as bromo-bridged $[Ag_2(\mu\text{-}Br)_2(\eta^1\text{-}S\text{–}H_2stsc)_2(PPh_3)_2]$ (**7a**), and sulfur-bridged $[Ag_2Br_2(\mu\text{-}S\text{–}H_2stsc)_2(PPh_3)_2]$ (**7b**) moieties (bond isomers) in the same unit cell similar to **1** or **2** (Fig. 4). No isomerism was observed with silver(I) chloride and only a sulfur-bridged dimer, $[Ag_2Cl_2(\mu\text{-}S\text{–}H_2stsc)_2(PPh_3)_2]$ (**8**) was formed. The central cores, $\{Ag(\mu\text{-}Br)_2Ag\}$ core of **7a**, and $\{Ag(\mu\text{-}S)_2Ag\}$of **7b**, form parallelograms with unequal Ag–Br or Ag–S distances as shown in Table 3. The Ag···Ag contacts are longer in the sulfur-bridged isomer **7b** (3.4223 Å) vis-à-vis that in bromo-bridged isomer **7a** (3.2021 Å), and this trend is reverse to that in analogous copper(I) complexes **1** and **2**. Complex **8** has a similar bonding pattern and structure as **7b**, however, the Ag···Ag contact in the former is shorter than in the latter complex (Table 3).

The substitution of methyl groups at N^1 ($H_2stscNMe$) has prevented dimerisation and instead of forming a dimer similar to **7** or **8**, mononuclear tetrahedral complexes, $[AgX(\eta^1\text{-}S\text{–}H_2stscNMe)(PPh_3)_2]\cdot 3CH_3CN$ (Br **9**, Cl **10**) have been obtained. Fig. 5 shows the molecular structure of compound **9** (Table 3).

4.3. Packing networks (*1–10*)

Both the halogen-bridged (**1a**, **2a**) and sulfur-bridged (**1b**, **2b**) moieties involve intramolecular imino hydrogen–halogen hydrogen bonding ($-N^2H\cdots X$) (Chart 2). Further, the 2-hydroxy group is engaged in intramolecular hydrogen bonding with azomethine nitrogen atom ($HO\cdots N^3-$). Two isomeric units, (**1a**, **1b** or **2a**, **2b**) are interlinked via amino hydrogen of **1b** or **2b** with sulfur atom of **1a** or **2a** ($-HN^1H\cdots S$), forming linear chains running along *a* axis. These linear chains show mutual phenyl–phenyl interactions (C–H···π, 2.892 Å, PPh_3) leading to the formation of 2D networks. The chloroform molecules present in the cavities form weak C–H···π interactions {$Cl_3C\text{–}H\cdots\pi$ (Ph–P)} (**1**, Fig. 6). Bond isomers (**1**, **2**) have shown stronger $-OH\cdots N^3$ hydrogen bonds, resulting in relatively weaker $-N^2H\cdots I$/$-N^2H\cdots Br$ hydrogen bonds (2.47–2.71 Å), (for other H-bonding parameters, see supplementary) and this may be responsible for the presence of bond isomerism in the complexes **1** and **2**.

The sulfur-bridged complex **4** has no intramolecular imino hydrogen–iodine ($-N^2H\cdots I$) hydrogen bonding unlike that in **1** or

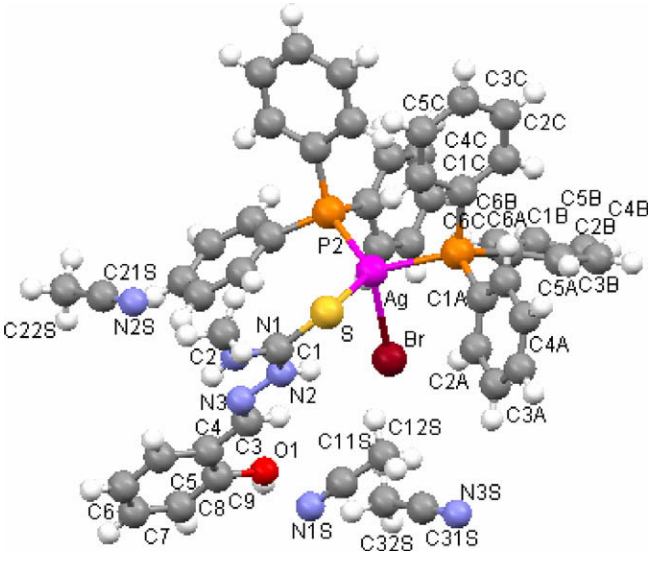

Fig. 5. Molecular structure of $[AgBr(\eta^1\text{-}S\text{–}H_2stscNMe)(PPh_3)_2]\cdot 3CH_3CN$ **9** (complex **10** has a similar structure).

Table 3
Selected bond distances (Å) and bond angles (°) of silver(I) complexes (**7**–**10**).

Complex no.	Ag–S	Ag–X	Ag–P	Ag–X–Ag	X–Ag–X	Ag···Ag
Halogen-bridged dimer						
7a[a]	2.5076(8)	2.7044(4) 2.8310(4) (Br)	2.4288(8)	70.643(11)	(109.358(11))	3.2021(5)
				Ag–S–Ag	S–Ag–S	
Sulfur-bridged dimers						
7b[a]	2.5491(8) 2.7811(8)	2.6563(4) (Br)	2.4238(8)	79.76(2)	100.24(2)	3.4223(5)
8[a]	2.6777(6) 2.8054(5)	2.5169(5) (Cl)	2.4169(5)	69.615(14)	106.043(17)	3.1041(5)
		Ag–P	Ag–X	P–Ag–P	P–Ag–X	P–Ag–S
Mononuclear complexes						
9[b]	2.6008(16)	2.4856(15) 2.4884(16)	2.8094(8) (Br)	121.90(6)	102.24(4) 103.43(4)	101.61(5) 123.93(5)
10[b]	2.5924(4)	2.4716(4) 2.4746(4)	2.7192(4) (Cl)	122.859(14)	102.440(14) 102.716(13)	100.634(13) 125.395(14)

[a] H_2stsc.
[b] $H_2stscNMe$.

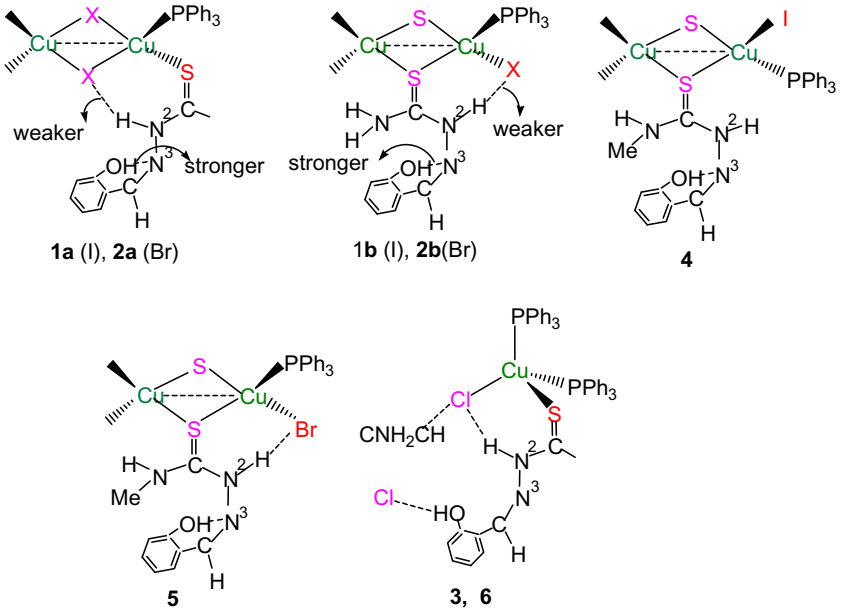

Chart 2.

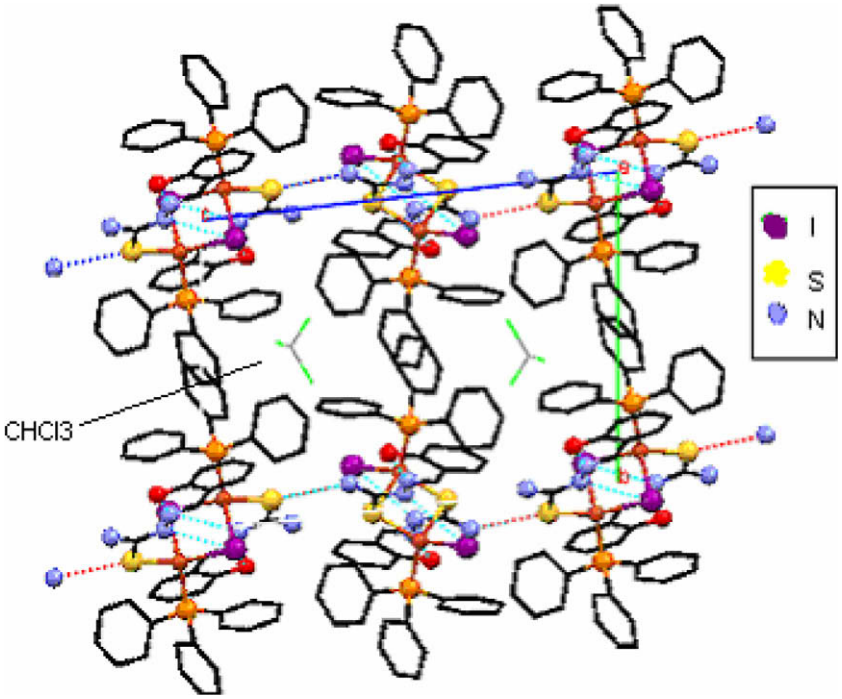

Fig. 6. 2D view of complex $[Cu_2Br_2(H_2stsc)_2(PPh_3)_2] \cdot CHCl_3$ **1** (complex **2** has a similar packing pattern).

2 (Chart 2). Further, the 2-hydroxy group is engaged in intramolecular hydrogen bonding with azomethine nitrogen atom (HO···N^3–). The CH_3CN molecules are engaged in hydrogen bonding with amino group (–CH_3N^1H···$NCCH_3$, 2.473 Å) as well as with the hydroxyl group interaction with π electrons of C≡N group (–HO···π). The dimers are further interlinked via phenyl–phenyl interactions of PPh_3 (C–H···π, 2.738 Å) along *a* axis resulting in the formation of 1D chains (Fig. 7). However, compound **5** showed intramolecular imino hydrogen–bromine (–N^2H···Br) as well as –N^3···HO hydrogen bonding (Chart 2). The CH_3CN molecules showed similar intermolecular CH_3N^1H···$NCCH_3$ (2.541 Å) and –HO···π interactions. In addition, it also showed interactions with the bromine atom (–Br···HCH_2CN, 2.989 Å) forming a linear chain along *a* axis (Fig. 8). These linear chains are further linked via phenyl–phenyl interactions (–CH···π, 2.7300 Å, PPh_3) resulting in a 2D polymeric network along *b* axis (see Supplementary data). The interactions of CH_3CN are clearly different in these two complexes (**4**, **5**).

The chlorine atom in $[CuCl(\eta^1\text{-}S\text{–}H_2stc)(PPh_3)_2]$ **3** is engaged in hydrogen bonding intramolecularly with imino hydrogen (–N^2H···Cl), and intermolecularly with hydroxyl hydrogen (–OH···Cl) and the resulting network entraps two acetonitrile molecules, the hydrogen atoms of which are involved in hydrogen

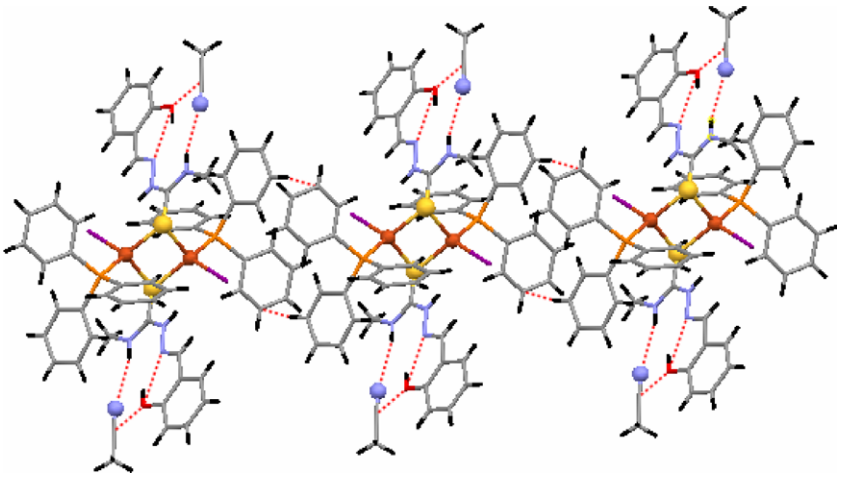

Fig. 7. Packing diagram of $[Cu_2I_2(\mu\text{-}S\text{–}H_2stscNMe)_2(PPh_3)_2] \cdot 2CH_3CN$ **4**.

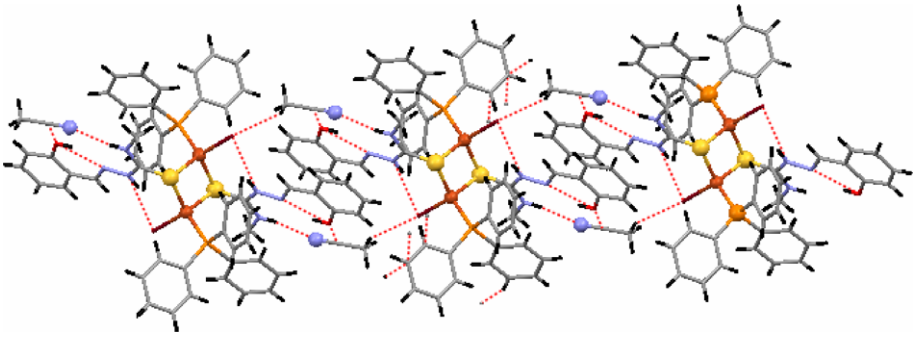

Fig. 8. Packing diagram of $[Cu_2Br_2(\mu\text{-}S\text{–}H_2stscNMe)_2(PPh_3)_2] \cdot 2CH_3CN$ **5**.

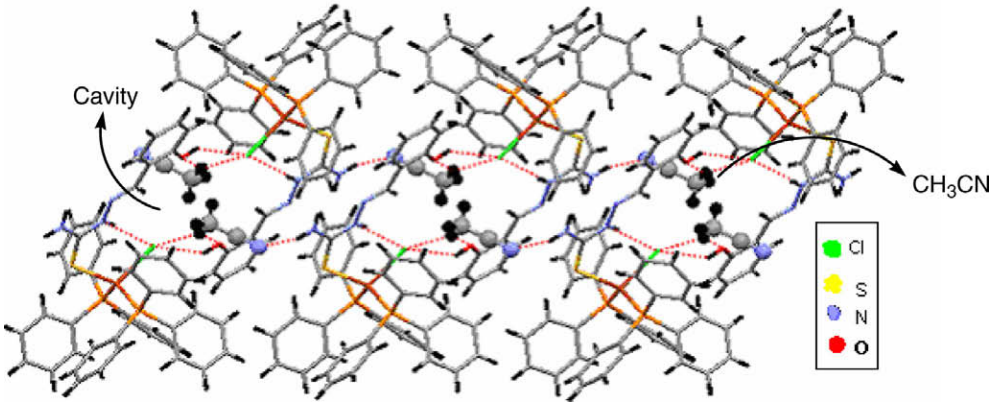

Fig. 9. Packing diagram of $[CuCl(\eta^1\text{-}S\text{–}H_2stsc)(PPh_3)_2] \cdot CH_3CN$ **3** (complex **6** showed similar packing pattern).

bonding with the chlorine atoms ($NCCH_2H\cdots Cl$).This dimer is further connected to the second dimer via amino hydrogen atoms ($-HN^1H\cdots NCCH_3$) along *a* axis, resulting in 2D polymeric network (Fig. 9). Complex **6** also showed similar interactions and formed a 2D network.

The packing diagram of compound **7** shows two crystallographically independent dimeric units, bromo-bridged dimer **7a**, and sulfur-bridged dimer **7b** in the same unit cell. In the sulfur-bridged (**7b**) and bromo-bridged isomeric units (**7a**) have similar type of intramolecular hydrogen bonding between imino hydrogen and halogen ($-N^2H\cdots Br$) as well as between azomethine nitrogen and hydroxyl oxygen atoms ($OH\cdots N^3-$). Two isomeric units are further linked via intermolecular hydrogen bonding between amino hydrogen of sulfur-bridged isomer **7b** with sulfur atom of bromo-bridged isomer **7a** ($-HN^1H\cdots S$), forming linear chains running along *a* axis. Two H-bonded acetonitrile molecules reside in the interstitial spaces are present in the cavity created between parallel chains and are involved in acetonitrile-terminal bromine interactions(C–H···Br) with terminal bromine (Fig. 10).

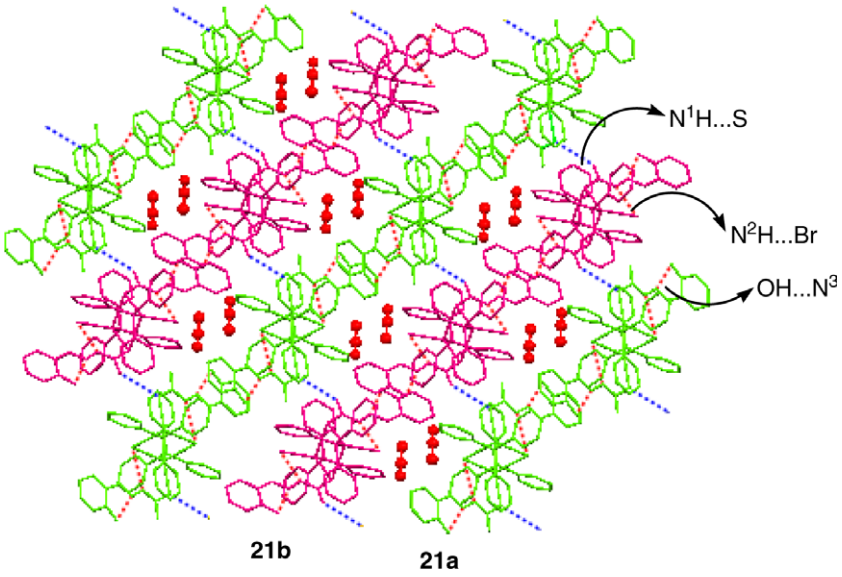

Fig. 10. 2D network of $[Ag_2Br_2(H_2stsc)_2(PPh_3)_2] \cdot 2CH_3CN$ **7** having alternate bromo-bridged (**7a**, green) and sulfur-bridged (**7b**, red) dimeric chains. (For interpretation of the references to color in this figure legend, the reader is referred to the web version of this article.)

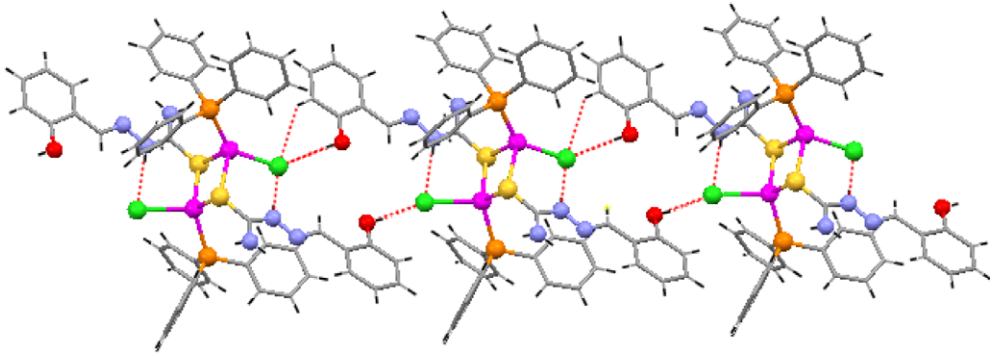

Fig. 11. 1D linear polymeric chain of complex $[Ag_2Cl_2(\mu\text{-}S\text{–}H_2stsc)_2(PPh_3)_2]$ **8**.

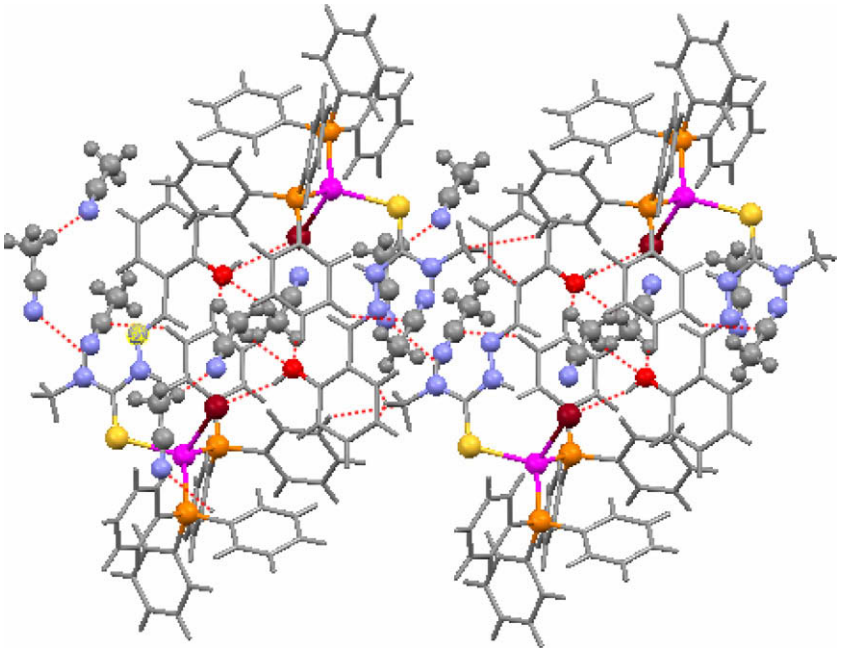

Fig. 12. Packing diagram of complex $[AgBr(\eta^1\text{-}S\text{–}H_2stscNMe)(PPh_3)_2] \cdot 3CH_3CN$ **9** (complex **10** shows similar packing pattern).

The sulfur-bridged silver(I) dimer **8** shows intramolecular hydrogen bonding between imino hydrogen and chlorine atoms ($-N^2H\cdots Cl$). The dimer units are further linked to each other by intermolecular OH···Cl and $Cl\cdots H_{Ph}$ hydrogen bonding, resulting in a linear polymeric 1D chain (Fig. 11).

The packing diagram of complex **9** reveals the presence of intramolecular $-N^2H\cdots Br$ hydrogen bonding. Two monomer molecules are interlinked via –HO···Br hydrogens generating a 20 membered cavity. The hydrogen atoms of methyl group at N^1 atom exhibit intermolecular interactions with phenyl ring of PPh_3 (–CH···π, 2.857 Å) and H_2stscNMe ligand (–CH···π, 2.761 Å) resulting in 2D network. Acetonitrile molecules are present in the cavity and are engaged in intermolecular hydrogen bonding with phenyl ring (–CH···π, 2.885 Å, PPh_3) and amino hydrogen atom ($-CH_3-N^1H\cdots NCCH_3$, 2.595 Å) (Fig. 12). Compound **10** shows similar interactions.

5. Solution phase behavior

It may be significant to understand the solution phase behavior of complexes **1**–**10** using ^1H and ^{31}P NMR spectroscopy. While ^1H NMR spectra of complexes reveal the presence of diagnostic $-N^2H$, $-N^1H_2$, –OH and phenyl ring protons of thiosemicarbazone and PPh_3, the ^{31}P NMR spectra reveal information about the state of the species in solution phase. The ^{31}P NMR spectra of **1**, **2** and **7** have revealed the presence of **2a**, **1b** isomers and both **7a** and **7b** isomers. It shows, depending on the medium ($CDCl_3$ for NMR and CH_3CN–$CHCl_3$ for crystal growth), the nature of dimeric specie can be different. For copper(I), **2b** converting to **2a** and **1a** converting to **1b**, but for silver(I), both **7a** and **7b** were present in the solution in $CDCl_3$. Similarly complex **8** reveals conversion of sulfur bridging into chloro-bridging. Complexes **3** and **6** remained unchanged in the solution phase. Sulfur-bridged dimers **4** and **5** showed a single signal each, with coordination shifts similar to the literature values [29].

6. Conclusion

The presence of 2-hydroxyphenyl (R^1) substituent at C^2 carbon (H_2stsc, R^1 = 2-HO–C_6H_4, $R^2 = R^3$ = H) appears to be responsible for the bond isomerism (μ-X, μ-S bridging) as exhibited by **1** and **2**. The introduction of methyl substituent at N^1 atom (H_2stscNMe) has led to the formation of only μ–S bridged dimers (**4**, **5**). Both H_2stsc and H_2stscNMe with copper(I) chloride form mononuclear complexes, **3** and **6**. Silver(I) bromide with H_2stsc formed **7** which again showed bond isomerism. Finally, silver(I) chloride with H_2stsc and silver(I) bromide/chloride with H_2stscNMe have formed μ-S bridged dimer (**8**, H_2stsc) or tetrahedral monomers (**9**, **10**, H_2stscMe). Lack of bond isomerism in **8** may be attributed to the presence of strong intermolecular OH···Cl hydrogen bonds which has served to stabilize sulfur bridging. The weak imino hydrogen–halogen hydrogen bonds in **1**, **2** and **7** appear to provide the necessary impetus for crossover of small energy barrier between μ-X and μ-S bridged complexes, leading to the bond isomerism.

Supplementary data

CCDC 683519, 683520, 683521, 713437, 713438, 713439, 683846, 683847, 713440 and 713441 contain the supplementary crystallographic data for **3**, **2**, **1**, **6**, **5**, **4**, **8**, **7**, **9** and **10**, respectively. These data can be obtained free of charge via http://www.ccdc.cam.ac.uk/conts/retrieving.html, or from the Cambridge Crystallographic Data Centre, 12 Union Road, Cambridge CB2 1EZ, UK; fax: (+44) 1223-336-033; or e-mail: deposit@ccdc.cam.ac.uk.

Acknowledgements

Financial assistance (SK) from CSIR (F. No. 9/254(159)/2005-EMR-I), New Delhi, is gratefully acknowledged. The authors thank Matthias Zeller of Youngstown State University, USA, for X-ray crystallography.

References

[1] B.K. Saha, R.K.R. Jetti, L.S. Reddy, S. Aitipamula, A. Nangia, Cryst. Growth Des. 5 (2005) 887.
[2] (a) B. Moulton, M.J. Zaworotko, Chem. Rev. 101 (2001) 1629; (b) M. Oh, C.A. Mirkin, Nature 438 (2005) 651.
[3] B. Sarma, S. Roy, A. Nangia, Chem. Commun. (2006) 1369.
[4] C. Zhang, E. Staunton, Y.G. Andreev, P.G. Bruce, J. Am. Chem. Soc. 127 (2005) 18305.
[5] T. Okubo, R. Kawajiri, T. Mitani, T. Shimoda, J. Am. Chem. Soc. 127 (2005) 17589.
[6] X.-Y. Wang, L. Wang, Z.-M. Wang, S. Gao, J. Am. Chem. Soc. 128 (2006) 674.
[7] A. Nangia, Curr. Opin. Solid State Matter Sci. 5 (2001) 115.
[8] J.A. McMohan, B. Moulton, R.D.B. Walsch, N. Rodriguez-Hornedo, M.J. Zaworotko, Cryst. Growth Des. 3 (2003) 909.
[9] M. Zaworotko, Angrew. Chem., Int. Ed. 39 (2000) 3052.
[10] R.D.B. Walsch, M.W. Bradner, S. Fleischman, L.A. Morales, B. Moulton, N. Rodriguez-Hornedo, M. Zaworotko, Chem. Commun. (2003) 186.
[11] M.J.M. Campbell, Coord. Chem. Rev. 15 (1975) 279.
[12] S.B. Padhye, G. Kauffman, Coord. Chem. Rev. 63 (1985) 127.
[13] D.X. West, S.B. Padhye, P.B. Sonawane, Struct. Bond. (Berlin Ger.) 76 (1991) 4.
[14] D.X. West, A.E. Liberta, S.B. Padhye, R.C. Chikate, P.B. Sonawane, A.S. Kumbhar, R.G. Yerande, Coord. Chem. Rev. 123 (1993) 49.
[15] J.S. Casas, M.S. Garcia-Tasende, J. Sordo, Coord. Chem. Rev. 209 (2000) 197.
[16] D.R. Smith, Coord. Chem. Rev. 164 (1997) 575.
[17] T.S. Lobana, S. Khanna, R. Sharma, G. Hundal, R. Sultana, M. Chaudhary, R.J. Butcher, A. Castineiras, Cryst. Growth Des. 8 (2008) 1203.
[18] R.K. Mahajan, I. Kaur, T.S. Lobana, Talanta 59 (2003) 101.
[19] R.K. Mahajan, I. Kaur, T.S. Lobana, Ind. J. Chem. 45A (2006) 639.
[20] R.K. Mahajan, T.P.S. Walia, Sumanjit, T.S. Lobana, Talanta 67 (2005) 755.
[21] L.S. Sarma, J.R. Kumar, C.J. Kumar, A.V. Reddy, Anal. Lett. 36 (2003) 605.
[22] K.J. Reddy, J.R. Kumar, C. Ramachandraiah, T. Thriveni, A.V. Reddy, Food Chem. 101 (2007) 585.
[23] M.A. Ali, M.E. Khalifa, S.E. Ghazy, M.M. Hassanien, Anal. Sci. 18 (2002) 1235.
[24] U. Abram, K. Ortner, R. Gust, K. Sommer, J. Chem. Soc., Dalton Trans. (2000) 735.
[25] K. Nomiya, K. Sekino, M. Ishiawa, A. Honda, M. Yokoyama, N.C. Kasuga, H. Yokoyama, S. Nakano, K. Onodera, J. Inorg. Biochem. 98 (2004) 601.
[26] M.B. Ferrari, F. Bisceglie, G. Pelosi, P. Tarasconi, R. Albertini, A. Bonati, P. Lunghi, S. Pinelli, J. Inorg. Biochem. 83 (2001) 169.
[27] D.X. West, J.S. Ives, J. Krejci, M.M. Salberg, T.L. Zumbahlen, G.A. Bain, A.E. Liberta, J. Valdes-Martinez, S. Hernadez-Ortiz, R.A. Toscano, Polyhedron 14 (1995) 2189.
[28] J. Garcia-Tojal, L. Lezama, J.L. Pizarro, M. Insausti, M.I. Arriortua, T. Rojo, Polyhedron 18 (1999) 3703.
[29] T.S. Lobana, R.J. Butcher, A. Castineiras, E. Bermejo, P.V. Bharatam, Inorg. Chem. 45 (2006) 1535.
[30] T.S. Lobana, A.P.S. Pannu, G. Hundal, R.J. Butcher, A. Castineiras, Polyhedron 26 (2007) 2621.
[31] W. Kaim, J. Rall, Angew. Chem., Int. Ed. Engl. 35 (1996) 43.
[32] R.J. Haines, R.E. Wittrig, C.P. Kubiak, Inorg. Chem. 33 (1994) 4723.
[33] J. Anekwe, A. Hammerschmidt, A. Rompal, B. Krebs, Z. Anorg. Allg. Chem. 632 (2006) 1057.
[34] E.I. Solomon, U.M. Sundaram, T.E. Machonkin, Chem. Rev. 96 (1996) 2563.
[35] K. Singh, J.R. Long, P. Stavropoulos, Inorg. Chem. 37 (1998) 1073.
[36] H. Araki, K. Tsuga, Y. Sasaki, S. Ishizaka, N. Kitamura, Inorg. Chem. 46 (2007) 10032.
[37] H.V.R. Dias, H.V.K. Diyabalanage, M.G. Eldabaga, O. Elbjeirama, MA. Rawashdeh-Omary, J. Am. Chem. Soc. 127 (2005) 7489.
[38] A.A. Mohamed, A. Burini, J.P. Fackler Jr., J. Am. Chem. Soc. 127 (2005) 5012.
[39] G. Brauer, Handbook of Preparative Chemistry, 2nd Ed., vol. 2, Academic Press, New York, 1965.
[40] XSCANS, Siemens Analytical X-ray Instruments Inc., Madison, WI, USA, 1994.
[41] International Tables for X-ray Crystallography, vol. C, Kluwer, Dordrecht, The Netherlands, 1995.
[42] G.X. Win, L.J. Farrugia, J. Appl. Crystallogr. 32 (1999) 837.
[43] G.M. Sheldrick, SADABS, Program for Empirical Absorption Correction of Area Detector Data, University of Gottingen, Germany, 1997.
[44] Bruker, SMART, SAINT and XREP, Area Detector Control, and Data Integration and Reduction Software, Bruker Analytical X-ray Instruments Inc., Madison, Wisconsin, USA, 1995.
[45] G.M. Sheldrick, SHELXL-97, Program for the Refinement of Crystal Structures, University of Gottingen, Germany, 1997.